Cancer Letters 440–441 (2019) 189–201

Contents lists available at ScienceDirect

Cancer Letters

journal homepage: www.elsevier.com/locate/canlet

Original Articles

Loss of TMEM126A promotes extracellular matrix remodeling, epithelial-to-mesenchymal transition, and breast cancer metastasis by regulating mitochondrial retrograde signaling

He-Fen Sun[a,b,**], Xue-li Yang[a,b], Yang Zhao[a,b], Qi Tian[c], Meng-Ting Chen[a,b], Yuan-yuan Zhao[a,b], Wei Jin[a,b,*]

[a] Department of Breast Surgery, Key Laboratory of Breast Cancer in Shanghai, Fudan University Shanghai Cancer Center, Shanghai, 200030, China
[b] Department of Oncology, Shanghai Medical College, Fudan University, Shanghai, 200030, China
[c] Department of Obstetrics and Gynecology, Ren Ji Hospital, School of Medicine, Shanghai Jiao Tong University, China

ARTICLE INFO

Keywords:
TMEM126A
Metastasis
ECM
ROS

ABSTRACT

TMEM126A is a mitochondrial transmembrane protein, and its functions in breast cancer progression remain unclear. In this study, via the iTRAQ assay using primary and metastatic breast cancer cell models, we found that TMEM126A expression decreased in metastatic cells. We further confirmed that low TMEM126A expression correlated with tumor progression and poor prognosis in patients. The downregulation of TMEM126A in breast cancer cell lines significantly enhanced the metastatic properties *in vitro* and *in vivo*, whereas its overexpression decreased the metastatic potential of cell lines. Mechanistic studies based on RNA-sequencing indicated that TMEM126A might regulate cell metastasis via ECM-receptor interaction, focal adhesions, and actin cytoskeleton, among other processes. Furthermore, the loss of TMEM126A activated extracellular matrix (ECM) remodeling and promoted epithelial-to-mesenchymal transition (EMT). Moreover, TMEM126A silencing induced reactive oxygen species (ROS) production and mitochondrial membrane potential depolarization. The ROS scavengers reversed ECM remodeling and EMT mediated by TMEM126A. Collectively, our findings show that the loss of TMEM126A induces mitochondrial dysfunction and subsequently metastasis by activating ECM remodeling and EMT. These findings suggest that TMEM126A is a novel suppressor of metastasis and that it can be a potential prognostic indicator for patients with breast cancer.

1. Introduction

Breast cancer is the second most common cancer in females and metastasis is the main cause of death among these patients [1,2]. Despite the progress in the treatment of primary breast cancers with surgery, chemotherapy, and radiotherapy, a large proportion of patients with distant metastasis remain uncured.

During recent years, accumulating data have indicated that mitochondria play a vital role in tumor initiation and progression [3–5]. Mitochondrial dysfunction has also been reported to be associated with the increase in the metastatic capability of cancer cells [6]. Thus, the recent progress in the understanding of molecular functions of mitochondria has prompted the development of strategies to treat metastatic tumors. There are several proteins located in the mitochondria; however, their functions and associated mechanisms in breast cancer remain unknown. Therefore, further studies on mitochondrial proteins involved in cancer metastasis can provide insights into the mechanism of metastasis.

In our present study, to screen mitochondrial proteins involved in breast cancer metastasis, we utilized iTRAQ labeling technology

Abbreviations: EMT, epithelial-to-mesenchymal transition; ECM, extracellular matrix; TMEM126A, transmembrane protein 126A; TMAs, Tissue microarrays; IHC, immunohistochemical; DMFS, distant metastasis-free survival; DFS, disease-free survival; OS, overall survival; TNBC, Triple-Negative Breast Cancer; mtROS, mitochondrial reactive oxygen species; MMP, mitochondrial membrane potential ; ; NAC, N-Acetyl-L-cysteine; FBS, Fetal bovine serum; PBS, Phosphate buffered saline; ER, estrogen receptor; PR, progesterone receptor; Her-2, human epidermal growth factor receptor 2; CI, confidence interval; MLR, mitochondrial located mRNA

* Corresponding author. Department of Breast Surgery, Key Laboratory of Breast Cancer in Shanghai, Fudan University Shanghai Cancer Center, Shanghai, 200030, China.

** Corresponding author. Department of Breast Surgery, Key Laboratory of Breast Cancer in Shanghai, Fudan University Shanghai Cancer Center, Shanghai, 200030, China.

E-mail addresses: sunhefen2006@163.com (H.-F. Sun), jinwei7207@163.com (W. Jin).

https://doi.org/10.1016/j.canlet.2018.10.018
Received 10 August 2018; Received in revised form 3 October 2018; Accepted 19 October 2018

followed by nanoscale high-performance liquid chromatography (nano-HPLC)-MS/MS using cell lines with different metastatic potentials. We identified differential protein expression between a parental cell line (MDA-MB-231) and its highly metastatic derivative (MDA-MB-231HM). Several of these proteins were previously validated to affect breast cancer metastasis or tumorigenesis [7–10]. In this study, TMEM126A, our candidate gene, was expressed at low levels, specifically 7-fold lower in MDA-MB-231HM cells compared to that in parental MDA-MB-231 cells. This result suggested that TMEM126A might be a metastasis suppressor.

Human TMEM126A (transmembrane protein 126A, also named OPA7) is encoded by a gene that is located on chromosome 11. It is a mitochondrial inner membrane protein consisting of two isoforms that are encoded by different transcript variants of this gene. Variant 1 consists of 195 amino acids and is predicted to contain four transmembrane domains with N− and C-terminal sequences on the outside of the membrane. Variant 2 has a shorter N-terminus than that of isoform 1 [11,12]. Further, defects and mutations in TMEM126A cause autosomal recessive optic atrophy [13,14]. TMEM126A has also been reported to bind to CD137 ligand (CD137L, 4-1BBL), inducing reverse signaling in macrophages. The knockdown of TMEM126A abolishes CD137L-induced tyrosine phosphorylation and cell adherence [15,16]. Based on our preliminary results, the aim of the present study was to elucidate the role of TEM126A in breast cancer metastasis. To the best of our knowledge, the present study is the first to show that TMEM126A can suppress breast cancer metastasis.

2. Material and methods

2.1. Cell culture

The cell lines were obtained from the Shanghai Cell Bank, Type Culture Collection Committee of Chinese Academy of Science (Shanghai, China). The highly metastatic cell line MDA-MB-231HM was developed from parental MDA-MB-231 cells in our laboratory via *in vivo* selection by four cycles of tail vein injections; we have a current patent application for this cell line (patent number: 200910174455.4). MDA-MB-231Bo, which also exhibits enhanced lung metastasis capacity, was obtained from Dr. Toshiyuki Yoneda (The University of Texas, Houston, TX). These cell lines were maintained in our laboratory and subjected to routine cell line quality examinations (e.g., morphology and *Mycoplasma* infection) by HD Biosciences every three months. The cells for experiments were passaged for less than six months. All cell lines were maintained under conditions specified by the provider, and were cultured in a 5% CO_2 incubator at 37 °C.

2.2. Study population

We used 241 primary breast cancer samples from patients with stages I to III invasive ductal carcinoma collected randomly at the Department of Breast Surgery in Fudan University Shanghai Cancer Center (FDUSCC, Shanghai, P.R. China) between August 2001 and March 2006. All cases had complete pathological diagnosis and follow-up records, and the histological grade was I to III. The clinical data included age, menstrual status, histological grade, tumor size, lymph node status, ER, PR, HER2 status, recurrence or metastasis time, and total survival time. The deadline for follow-up information was August 2013, with a median follow-up of 98 months. The patients were treated according to the standards used during surgery and those who were not found to be fit for surgery received adjuvant chemotherapy with different regimens for four to six cycles and/or hormone therapy (if required), according to the standard therapy during surgery. This study was approved by the Ethics Committee of FDUSCC, and each participant provided signed informed consent.

2.3. Tissue microarrays, immunohistochemical (IHC) staining, and IHC variable evaluation

Tissue microarrays (TMAs) were obtained from archived formalin-fixed, paraffin wax-embedded carcinomas samples from patients, as described in our previous study [8]. The TMAs composed of duplicate cores from different areas of the same tumor to compare staining patterns. The immunohistochemical (IHC) analysis was done essentially as described previously [17]. A total of 250 breast tumor specimens were included in the IHC analysis. The IHC variables were scored semi-quantitatively according to a previous study [18]. The details of TMAs construction, IHC staining, and IHC variable evaluation are presented in the Supplementary Methods.

2.4. Quantitative real-time PCR

Briefly, the total RNA was extracted using TRIzol reagent (Invitrogen Corporation) and reverse transcribed using the PrimeScript RT Reagent Kit (Perfect Real Time; TaKaRa Biotechnology). The real-time polymerase chain reaction (PCR) was performed with SYBR Premix Ex Taq (TaKaRa Biotechnology) using ABI Prism 7900 (Applied Biosystems). The sequence of primers used in this study is listed in Supplementary Table S1.

2.5. Plasmids and shRNA

Human TMEM126A cDNA was subcloned from the breast cancer cell line MDA-MB-231 into the pCDH-CMV-MCS-EF1-Puro lentiviral vector with the Flag tag. The cloned primer sequence was as follows:

Forward primer: 5′—CCGgaattc GCCACC ATG GAC TAC AAG GAC GAT GAT GAC AAG CTC GAT GGA GGA ATGGAAAATCATAAATC CAA-3′ Reverse primer: 5′-CGCggatcc TCAGTGAATTTCTTTGCCAG-3′.

TMEM126A shRNAs and the negative control were purchased from GeneChem and expressed in the pGIPZ backbone. The target sequences were as follows:

V3LHS_351007 mature antisense: ATGCTGAAAACATAGTCTG.
V3LHS_351009 mature antisense: TTGTCACATTCAAGATGCG.
V3LHS_351010 mature antisense: TTTAATCCAACATAAACCG.

2.6. Lentivirus packaging and infection

Briefly, 293T cells were co-transfected with the lentiviral vectors pCDH (or pGIPZ) and the packaging vectors psPAX2 and pMD2G. After 48 h, viral culture supernatants were collected, filtered, and added to the cells. The cells were incubated with virus and polybrene (Sigma-Aldrich) added at a working concentration of 8 mg/mL for 12 h, and then medium containing FBS was added. After 24 h, the infected cells were subjected to selection with 2 mg/mL puromycin for one week.

2.7. Western blot analysis

Whole-cell lysates were obtained using Pierce T-PER (Tissue Protein Extraction Reagent; Thermo Fisher Scientific Inc.) with protease inhibitor cocktail tablets and phosphatase inhibitors (Roche). The concentration of proteins was determined using the BCA Protein Assay Kit (Solarbio). In total, 30 mg of cell lysates was resolved by sodium dodecyl sulfate-polyacrylamide gel electrophoresis (SDS-PAGE) and transferred on to polyvinylidene fluoride membranes (Millipore). The membranes were blocked with 5% milk or 5% BSA, and then incubated with primary antibodies, followed by HRP-conjugated secondary antibodies. Immunoreactive bands were identified using chemiluminescent substance, according to the manufacturer's instructions, and quantified by densitometry. The antibodies used in this study are listed in Supplementary Table S2.

2.8. Transwell assays

Cells (5×10^4 cells/well for the migration assay and 1×10^5 cells/well for the invasion assay) were plated in the top chambers of non-coated membranes or Matrigel-coated Transwell chambers (BD Biosciences) in 200 μL of medium without FBS. Medium supplemented with 20% serum was used as a chemoattractant in the bottom chamber. After incubation for 15–20 h, the cells were fixed with 40% methanol and stained with 0.25% crystal violet. The cells that did not migrate through the pores were removed and the migrating cells were imaged and counted.

2.9. Kinetic wound-healing assay

Cells were plated on 96-well plates (Essen ImageLock, Essen Instruments) at a concentration of 3.6×10^4/100 μL of medium, and a wound was scratched with a wound scratch maker (Essen Instruments). Wound confluence was monitored with a Live-Cell Imaging System and software (Essen Instruments) every 4 h for 48 h by comparing the mean relative wound density of at least three biological replicates for each experiment.

2.10. Immunofluorescence

MCF10-Ca1h (pGIPZ and shT126A) stable cell lines were seeded on coverslips overnight, fixed with 4% paraformaldehyde for 30 min at room temperature, permeabilized with 0.5% triton X-100 for 5 min at 4 °C, and incubated with FN-1 (Proteintech, 1:200, Rabbit) or N-CAD (BD, 1:200, Mouse) primary antibodies overnight at 4 °C. The slides were then incubated with Alexa 594-conjugated (red, Invitrogen) secondary antibodies for 30 min at room temperature, and then incubated with 4′,6-diamidino-2-phenylindole (DAPI) for 10 min. Images were captured with a confocal laser microscope (Leica TCS SP5 II). At least 100 cells were analyzed per group.

2.11. Cell adhesion assay

Cells were harvested with trypsin and washed twice with serum-free medium, The cells (1×10^5 cells/well) were then seeded onto serum-depleted medium for the indicated times in 24-well plates precoated with a uniform substrate layer of a single ECM protein, specifically, collagen I, collagen IV, fibrinogen, fibronectin, or laminin (cell adhesion ECM array, Cell BioLabs, INC.). Each well was gently washed 4–5 times with PBS and stained with the Cell Stain Solution; the extraction solution was added and the OD at 560 nm was measured using a plate reader.

2.12. Mitochondrial membrane potential assay

Tumor cells plated in phenol red-free growth medium were treated with 1 mg/mL JC-1 dye for 30 min at 37 °C and analyzed by fluorescence-activated cell sorting (FACS). Red or green JC-1 fluorescence signals were resolved by detection in the FL1 and FL3 channels, respectively. The loss of mitochondrial membrane potential was measured by a reduction in the red/green fluorescence intensity ratio.

2.13. Mitochondrial reactive oxygen species

Mitochondrial-specific superoxide production was measured by labeling live cells with MitoSOX-Red (Invitrogen). The cells were incubated with 5 mmol/L MitoSOX-red for 20 min at 37 °C in serum-free DMEM, washed twice with Dulbecco PBS, and then immediately analyzed by FACS.

2.14. Mice and tumor studies

All animal experiments were performed in accordance with the guidelines of the Institutional Animal Care and Use Committee of Fudan University under approved protocols. For cell metastasis analysis, 3×10^5 cells labeled with GFP/luciferase were washed in serum-free DMEM and injected intravenously into female BALB/c nude mice (N = 6) to study lung metastasis. After 4–6 weeks, noninvasive bioluminescence imaging (BLI) was performed to quantify metastasis using an *in vivo* imaging system. For cell growth, 2×10^6 cells/100 μL were injected into the mammary fat pad of 8-week-old female nude mice. The tumor volume was measured twice a week for 4–6 weeks with electronic calipers, and then the tumors were harvested and weighed.

2.15. Statistical analyses

All data are reported as mean ± standard deviation (SD) as indicated in the figure legends. The data were analyzed using PRISM 5.0 (GraphPad Software Inc.) and SPSS 18.0 software (SPSS). Comparisons between two groups were performed by the student's *t*-test (two-tailed). The cumulative survival time was calculated by Kaplan-Meier method (log-rank test). The univariate and multivariate analyses were based on Cox proportional hazards regression model. The results with P value < 0.05 were considered statistically significant.

3. Results

3.1. TMEM126A expression is downregulated in highly metastatic breast cancer cells

In our previous study, we analyzed a large number of candidate genes that were found to be differentially expressed between the highly metastatic sub-line MDA-MB-231HM and its parental cell line MDA-MB-231 (Fig. 1A). The expression of TMEM126A, one of the candidate genes, was downregulated by 7-fold in MDA-MB-231HM compared with that in MDA-MB-231 cells (Fig. 1B and C). A panel of breast cancer cell lines was also evaluated to validate the general expression pattern of TMEM126A. In accordance with the iTRAQ results, the expression of TMEM126A mRNA and protein was generally observed in luminal breast cancer cells (MCF-7, T47D), which are considered weakly metastatic, but was downregulated in basal-like breast cancer cells (Hs-578T, MDA-MB-468, and MDA-MB-231). In particular, the highly metastatic cell lines (MDA-MB-231HM and MDA-MB-231Bo) exhibited higher decreases in TMEM126A expression (Fig. 1D and E).

In addition, the Oncomine expression analysis revealed that TMEM126A was downregulated in metastatic tissue compared with that in the primary tumor counterpart (Fig. 1F). We also examined the expression of TMEM126A in 25 pairs of fresh samples including normal breast tissues, primary tumor tissues, and metastatic lymph nodes. The results indicated that TMEM126A expression was significantly reduced in the metastatic lymph nodes compared with that in the primary cancer, which is consistent with the results of the Oncomine analysis (Fig. 1G).

Moreover, we evaluated the prognostic value of TMEM126A using an online Kaplan-Meier plot tool for survival analysis. In the entire patient cohort, high TMEM126A expression had a positive effect on distant metastasis-free survival (DMFS) (Fig. 1H). We also evaluated the correlation between prognosis and TMEM126A expression in other cancer types, including lung, gastric, and ovarian cancers by online Kaplan-Meier plotting; however, the disease-free survival (DFS) and DMFS data of other cancer type were lacking in the database and therefore we used overall survival (OS) to a substitute. The results showed that OS negatively correlated with TMEM126A expression in lung and ovarian cancers, but positively correlated with that in gastric cancer (Supplementary Figs. S1A–C).

In addition, we also analyzed the correlation between breast cancer

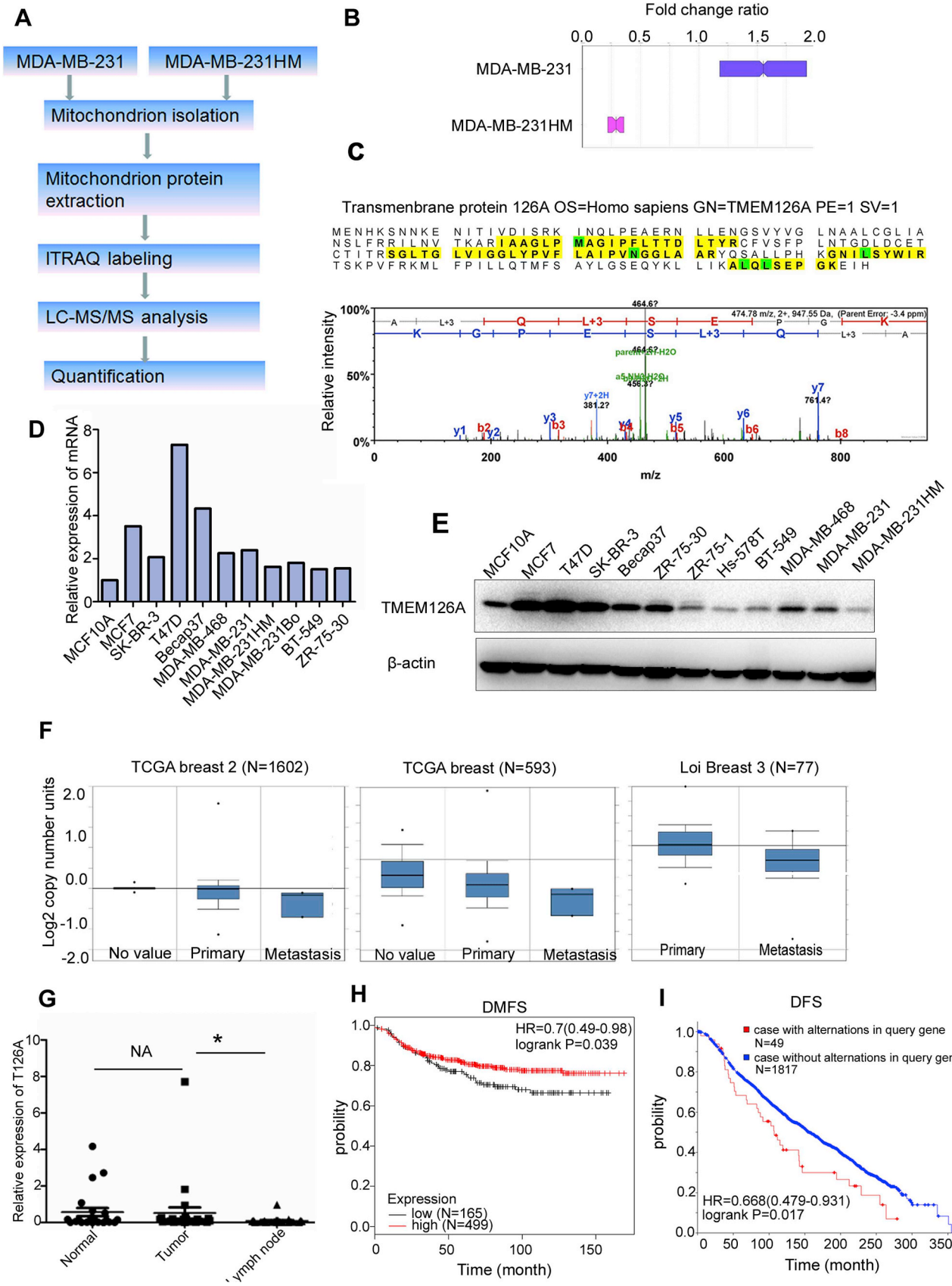

(caption on next page)

Fig. 1. TMEM126A expression is down-regulated in highly metastatic breast cancer cells.
A, Schematic overview of protein quantitative analysis approaches and three biological replicates were conducted per group. B, Relative expression of TMEM126A in MDA-MB-231 and MDA-MB-231HM.
cells. C, Peptide sequence and spectrum of TMEM126A obtained by mass spectrometry. D, Relative expression of *TMEM126A* mRNA in breast cancer cell lines based on real-time PCR. E, Relative expression of TMEM126A in breast cancer cell lines assessed by western blotting. F, Oncomine-based box plots of TMEM126A expression in primary tumors and metastasis sites based on TCGA breast (N = 593), TCGA breast 2 (N = 1602), and Loi breast 3 (N = 77) databases. G, *TMEM126A* mRNA expression in paired normal breast, breast cancer, and lymph node tissues based on real-time PCR. H, Distant metastasis-free survival (DMFS) analysis of TMEM126A expression in breast cancer samples using an online Kaplan-Meier plotter. I, Disease-free survival (DFS) analysis, based on TMEM126A expression, in cBioPortal for Cancer Genomics of breast cancer(METARIC, Nature 2012 & Nat common 2016, 2509 samples).

prognosis and TMEM126A expression using cBioPortal. We found that the cases with altered TMEM126A expression had a better DFS than those without gene alternations, and significant deletions in TMEM126A indicated high risk of breast cancer metastasis (Fig. 1I and Supplementary Fig. S1D). Overall, these data suggest that TMEM126A might play different roles in multiple cancer types.

3.2. Low TMEM126A expression correlates with poor prognosis

To determine the clinical relevance of the aforementioned findings in human breast cancer tissues, we examined the expression of TMEM126A in TMAs containing 250 breast tumor specimens by the IHC analysis (Fig. 2A). Notably, low TMEM126A expression correlated with poor DFS in all datasets. In luminal B and TNBC (Triple-Negative Breast Cancer) subtypes, low TMEM126A expression was also associated with poor DFS, but not in Her2$^+$ and luminal A subtypes (Fig. 2B–F).

We further analyzed the relationship between alterations in TMEM126A protein expression and clinicopathological characteristics in patients with breast cancer. The results showed that the ER status was related to the expression of TMEM126A (ER- 57.1% vs. ER+ 42.9%, $P = 0.017$). An increase in the number of metastasis lymph nodes was associated with low TMEM126A expression (LN = 0: 61.9% vs. 59.3%, 1 ≤ LNs ≤4: 19.8% vs. 32.2%, LNs ≥5: 18.3% vs. 9.6%; $P = 0.032$). Low TMEM126A expression was associated with distant metastasis (25.4% vs. 14.8%, $P = 0.041$). TMEM126A expression had no association with local recurrence ($P = 0.651$). Moreover, other clinical characteristics, such as age, histological grade, tumor size, PR, HER2, and local recurrence, were not related to the expression of TMEM126A (Table 1).

Moreover, the univariate analysis indicated that low TMEM126A expression at diagnosis was associated with a higher risk of disease relapse (Table 2). Additional multivariate COX analysis presented a similar trend (Table 2). These findings confirmed that TMEM126A might have a crucial role in breast cancer.

3.3. Loss of TMEM126A promotes breast cancer cell metastasis in vitro and in vivo

To further investigate the role of TMEM126A in tumor metastasis, we constructed several TMEM126A overexpressing and knockdown stable cell lines. The western blot analysis demonstrated that TMEM126A was successfully overexpressed in cell lines such as Hs-578T, MDA-MB-231HM, MCF10A, MCF10-Ca1h, and MCF10-Ca1a. Moreover, both shRNA constructs markedly reduced TMEM126A protein levels in MDA-MB-231, ZR-75-30, and MCF10-Ca1h cells (Fig. 3A). Further, we evaluated the effect of TMEM126A on the malignant phenotype of breast cancer cells *in vitro*. The results showed that the

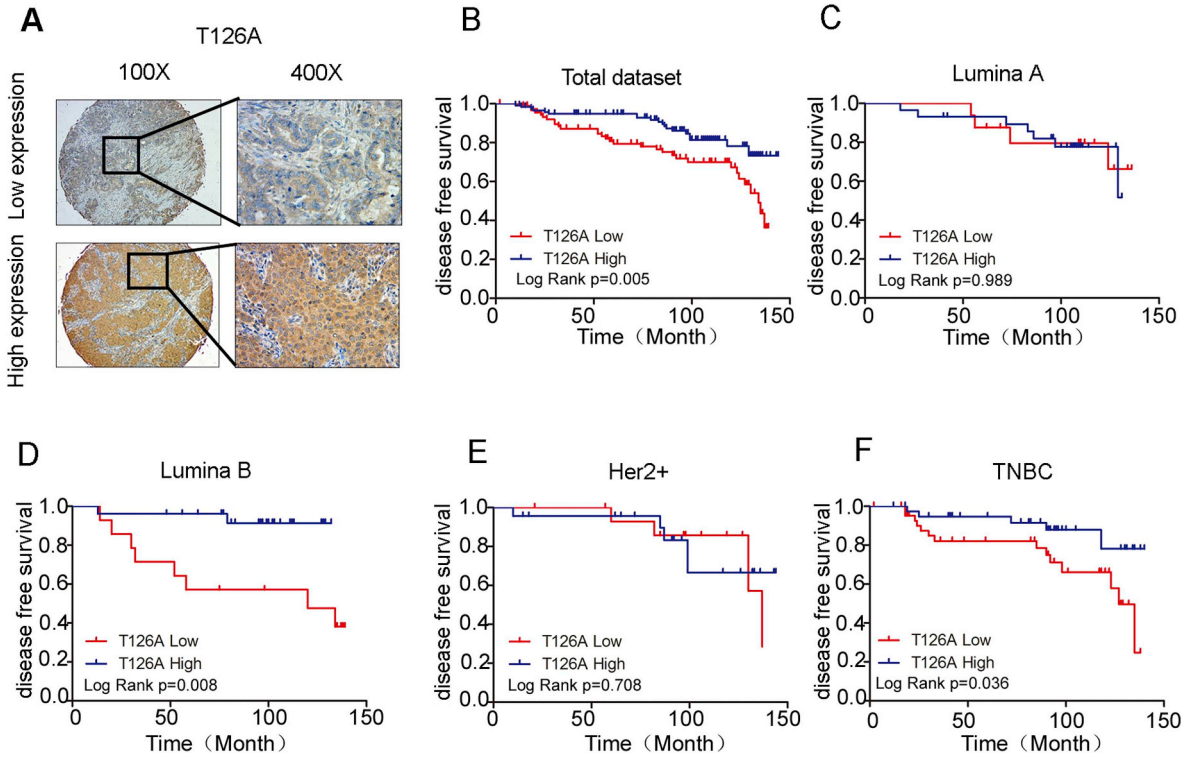

Fig. 2. Low TMEM126A expression correlates with poor prognosis for patients with breast cancer.
A, Representative immunohistochemical images of TMEM126A protein expression are shown at magnifications of 100 × and 400 × . B—F, Cumulative disease-free survival (DFS) curves based on TMEM126A expression, using the data from all the patients, as well as those with luminal A, luminal B, Her2$^+$, and TNBC subtypes.

Table 1
Alteration of TMEM126A protein expression levels in relation to clinicopathological characteristics in breast cancer patients.

Variables		TMEM126A				total		
		Low expression		High expression				
		n = 105		n = 136		n = 241		
		No.	%	No.	%	No.	%	*p*
Age(years)	10–49	53	50.5	63	46.3	116	48.1	0.522
	50–85	52	49.5	73	53.7	125	51.9	
Marital status	Married	44	41.9	62	45.6	106	44	0.568
	Not married	61	58.1	74	54.4	135	56	
Grade	I	2	2.3	3	2.5	5	2.4	0.574
	II	56	65.1	86	71.7	142	68.9	
	III	28	32.6	31	25.8	59	28.6	
Tumor size (cm)	≤2	51	48.6	60	45.1	111	46.6	0.181
	> 2 and ≤ 5	46	43.8	69	51.9	115	48.3	
	> 5	8	7.6	4	3.1	12	5	
No. of metastatic LNs	0	78	61.9	67	59.3	145	60.2	**0.032**
	1–4	25	19.8	37	32.2	62	25.7	
	≥5	23	18.3	11	9.6	34	14.1	
	Positive	43	41.3	50	37	93	38.9	
ER	Negative	69	65.7	68	50.4	137	57.1	0.017
	Positive	36	34.3	67	49.6	103	42.9	
PR	Negative	80	76.2	95	71.4	175	73.5	0.408
	Positive	25	23.8	38	28.6	63	26.5	
HER2	Negative	67	63.8	79	58.5	146	60.8	0.405
	Positive	38	36.2	56	41.5	94	39.2	
Metastasis	Negative	94	74.6	98	85.2	192	79.7	**0.041**
	Positive	32	25.4	17	14.8	49	20.3	
Recurrence	Negative	114	90.5	102	87.7	216	89.6	0.651
	Positive	12	9.5	13	11.3	25	10.4	

Notes: LNs: lymph nodes ER: estrogen receptor; PR: progesterone receptor; Her-2: human epidermal growth factor receptor 2; CI: confidence interval.

Table 2
Univariate and multivariate survival analysis of TMEM126A expression in breast cancer patients.

Variables	Univariate analysis		Multivariate analysis	
	HR (95% CI)	P-Value	HR (95% CI)	P-Value
Age (years)	0.978 (0.561–1.704)	0.937	1.007 (0.491–2.065)	0.986
menstrual status	1.757 (0.984–3.138)	0.057	1.811 (0.813–4.034)	0.146
Grade	2.553 (1.443–4.516)	0.001	2.728 (1.423–5.231)	0.003
Stage	1.499 (1.013–2.217)	0.043	0.709 (0.358–1.405)	0.97
Tumor size (cm)	1.539 (0.975–2.431)	0.064	1.335 (0.765–2.331)	0.309
LN status	2.150 (1.220–3.789)	0.008	2.515 (1.024–6.175)	0.044
ER	0.903 (0.514–1.587)	0.724	2.375 (0.927–6.083)	0.072
PR	0.452 (0.212–0.964)	0.04	0.195 (0.067–0.572)	0.03
Her2	0.940 (0.531–1.664)	0.833	0.826 (0.405–1.685)	0.6
T126A	0.457 (0.257–0.811)	0.007	0.397(0.202–0.779)	0.007

Notes: ER: estrogen receptor; PR: progesterone receptor; Her-2: human epidermal growth factor receptor 2; CI: confidence interval.

overexpression of TMEM126A significantly suppressed the migration and invasion of MDA-MB-231HM, MCF10-Ca1a, and Hs-578T cells, and that knockdown notably promoted the migration and invasion of ZR-75-30 and MDA-MB-231 cells (Fig. 3B–E). Moreover, TMEM126A depletion resulted in the migration of MDA-MB-231 and ZR-75-30 cells, based on the wound-healing assay (Fig. 3F and G). These results suggest the potential role of TMEM126A in suppressing the metastatic properties of tumor *in vitro*.

To examine whether TMEM126A affects metastasis *in vivo*, we generated three groups of mouse models. We first labeled TMEM126A-knockdown MDA-MB-231 cells, and TMEM126A-overexpressing MDA-MB-231HM and MCF10-Ca1a cells with a retroviral construct expressing a GFP/luciferase fusion protein [19]. The mice were then monitored by noninvasive BLI 4–6 weeks after the intravenous administration of cells into nude mice. Our results demonstrated that the upregulation of TMEM126A significantly decreased lung metastasis and that lung metastasis was elevated after TMEM126A downregulation in MDA-MB-231 cells (Fig. 3H and I). These findings indicated that TMEM126A expression suppresses breast cell metastasis *in vitro* and *in vivo*.

We also assessed the function of TMEM126A in cell cycle progression and proliferation. The cell cycle analysis showed that TMEM126A knockdown did not affect cell cycle distribution in MDA-MB-231 cells (Supplementary Fig. S2A and S2B). The upregulation of TMEM126A also did not alter the proliferation of MCF10-Ca1h and MCF10-Dics cells (Supplementary Fig. S2C). To further determine whether TMEM126A regulates the proliferation of breast cancer cell *in vivo*, cells (2×10^6 cells/mouse; MCF10-Ca1a pCDH vs. TMEM126A and MCF10-Dics pCDH vs. TMEM126A) were seeded into the fat pad of nude mice by subcutaneous injection, and the tumors were allowed to form for 4–6 weeks (Supplementary Figs. S2D and S2E). The results showed that TMEM126A had no function in tumor growth *in vivo*.

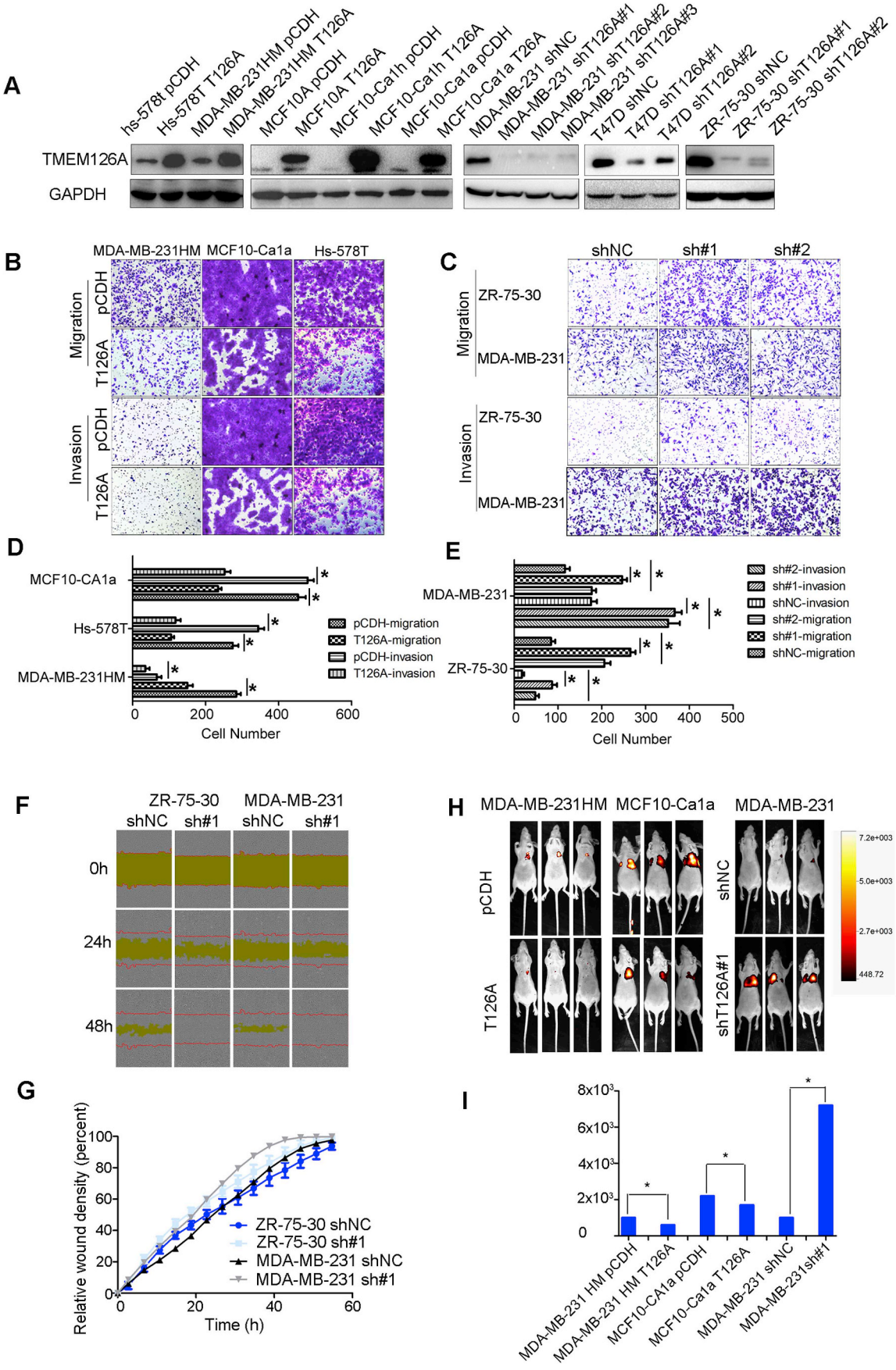

(caption on next page)

Fig. 3. Loss of TMEM126A expression promotes breast cancer cell metastatic properties *in vitro* and *in vivo*.
A, TMEM126A expression was analyzed after overexpression in Hs-578T, MDA-MB-231HM, MCF10A, MCF10-Ca1h, and MCF10-Ca1a cells, as well as after stable knockdown in MDA-MB-231, ZR-75-30, and MCF10-Ca1h cells, by western blotting. B-E, Cell migration and invasion in cell lines with TMEM126A overexpression and knockdown were evaluated by the transwell assay *in vitro*; B and C, Photos of representative fields (magnification, 100 ×) of invasive cells; D and F, Histograms depicting the results. Statistical analysis was performed by the student's *t*-test (N = 3). Error bars, SD. $^*P < 0.05$ compared with control. F and G, Effects of TMEM126A on the migration of MDA-MB-231 and ZR-75-30 cells based on the wound-healing assay. The red lines indicate the initial scratch wound location and the yellow area shows the scratch wound mask. Images were captured every 4 h after wounding. H, Bioluminescent images (BLI) of three representative mice in each group 4–6 weeks after injection with TMEM126A-overexpressing MDA-MB-231, MCF10-Ca1a, and TMEM126A cells or MDA-MB-231 TMEM126A-knockdown cells. I, Maximum BLI signals of each group. (For interpretation of the references to color in this figure legend, the reader is referred to the Web version of this article.)

3.4. Loss of TMEM126A promotes cell adhesion via ECM remodeling and cytoskeletal reorganization

To identify the mechanism underlying TMEM126A-mediated metastasis, we performed RNA-sequence using TMEM126A-knockdown MDA-MB-231 cells and TMEM126A-overexpressing MCF10-Ca1a cells combining bioinformatic analysis to survey the potential target genes and pathways. The KEGG pathway enrichment analysis revealed several pathways that were altered, such as ECM-receptor interaction, cell adhesion molecules, TGFβ signaling, focal adhesion, and regulation of the actin cytoskeleton (Fig. 4A). The GO enrichment analysis indicated that the expression of genes involved in cell adhesion, collagen catabolic process, cell-matrix adhesion, extracellular matrix structure components, and focal adhesion were significantly altered (Fig. 4B–D).

To determine the pathways involved in TMEM126A-mediated metastasis, we examined the expression of candidate genes by real-time PCR and western blotting. The results showed that the deletion of TMEM126A significantly increased the expression of mRNA-encoding ECM molecules, such as LAMA4, DAG1, ITGA1, LAMA3, ITGB1, CSF1, and CDL6A7. With TMEM126A overexpression, the mRNA expression of *DAG1*, *ITGB1*, and *LAMA5* was downregulated (Fig. 4E). These results indicate that TMEM126A might play a crucial role in ECM remodeling.

The results of GO and KEGG enrichment analyses suggested that TMEM126A functions in cell adhesion; therefore, we performed ECM adhesion assays with TMEM126A-knockdown cells. The results showed that low expression of TMEM126A in MDA-MB-231, MCF10-Ca1h, and ZR-75-30 cells enhanced cell adhesion to ECM proteins, such as fibronectin, collagen I, collagen IV, and fibrinogen (Fig. 4F).

We also examined other signaling pathways such as the CD137L reverse signal and TGF-β pathways. Through IP-immunoblotting analysis, we found that TMEM126A is associated and co-localizes with CD137L; however, the loss of TMEM126A did not alter the phosphorylation of p65 and p105, downstream of the CD137L reverse signal. The separation of cell membrane and cytoplasmic compartments and activation of signaling via treatment with CD137-Fc also indicated that TMEM126A does not alter the subcellular localization or downstream signaling of CD137L (Supplementary Figs. S2A–E). Our results also showed that TMEM126A does not regulate the expression or localization of *p*-SMAD3 (Supplementary Figs. S2F and S2G).

3.5. Loss of TMEM126A mediates epithelial-to-mesenchymal transition to regulate cell migration

Cell invasion is the crucial primary step of cancer cell metastasis; as cancer cells become more invasive, they develop altered affinity for their ECM. This phenotypic change is followed by ECM remodeling, cytoskeletal organization, and cell adhesion to the ECM. The cells escaping from the primary cancer site require advanced motility and migration. Epithelial-to-mesenchymal transition (EMT) might be the underlying mechanism for this process, which is accompanied by diminished cell-cell adhesions and strengthened cell-ECM adhesions.

It is not clear whether TMEM126A regulates the cell cytoskeleton; therefore, we detected alterations in the cytoskeleton by performing F-actin staining of MCF10A (shNC vs sh#1 or sh#2), MDA-MB-231HM (pCDH vs T126A), and MCF10-Ca1a (pCDH vs T126A) cells. The deletion of TMEM126A in MCF10A cells resulted in a significantly elongated cytoskeleton indicative of EMT. In MDA-MB-231HM and MCF10-Ca1a cells, the upregulation of TMEM126A notably suppressed the length and number of pseudopodia. These results suggest that TMEM126A might regulate cell migration via cytoskeletal rearrangements (Fig. 5A and B).

Further, F-actin staining indicated that the depletion of TMEM126A promoted EMT in MCF10A cells. In addition, FN-1, one of the most important components of the ECM, is also an important marker of EMT. To further investigate whether the loss of TMEM126A mediates EMT in breast cancer cells, we examined the level of associated markers after creating stable overexpression and knockdown cell lines. The results showed that TMEM126A overexpression significantly decreased the expression of FN-1 and N-cadherin, and marginally upregulated the expression of E-cadherin and vimentin. We also validated the results using ZR-75-30 and MDA-MB-231HM cells. The depletion of TMEM126A notably elevated FN-1 and N-cadherin expression (Fig. 5C and D). We further confirmed the expression of FN-1 and N-cadherin by performing immunofluorescence assays in TMEM126A-depleted MCF10-Ca1h, which showed similar results (Fig. 5E).

3.6. ROS scavenger reverses TMEM126A-mediated EMT and ECM reprogramming

TMEM126A is a mitochondrial protein that resides in the inner membrane; we thus determined whether TMEM126A affects mitochondrial function. We verified if the loss of TMEM126A potentiates mitochondrial reactive oxygen species (mtROS) generation and the disruption of mitochondrial membrane potential (MMP). We also analyzed the level of mtROS generation and MMP in MCF10-Ca1h and MCF10-Dics cells. The results showed a significant loss of MMP and an increase in ROS production in TMEM126A-downregulated cells compared with those in the control cells (Fig. 6A–D). These results indicated that the loss of TMEM126A results in mitochondrial metabolic dysfunction, such as the disruption of MMP and the generation of mtROS.

To further confirm that mitochondrial dysfunction affects ECM remodeling and cell adhesion and migration, cells were incubated with an ROS scavenger N-acetyl-L-cysteine (NAC) for 24 h to determine whether this treatment can restore EMT and ECM remodeling. The results demonstrated that the ROS scavenger can significantly reduce the level of FN-1 and N-cadherin in the cells; however, the knockdown of TMEM126A upregulated their expression compared with that in control cells (Fig. 6E and F). In MCF10-Ca1h cells, we also found that the ROS scavenger significantly suppressed the expression of ECM molecules, such as LAMA4, DAG1, ITGA1, LAMA3, ITGB1, CSF1, and CDL6A7 (Fig. 6G).

4. Discussion

TMEM126A has been reported to be related to optic atrophy. Herein, the present study is the first to demonstrate that it suppresses breast cancer metastasis, but has negligible effect on cell proliferation *in vivo* and *in vitro*. In this study, we examined the expression of TMEM126A in a TMA from patients with breast cancer, and the results showed that the low expression of TMEM126A was related to poor DFS (Fig. 2B–F). The data analysis using cBioPortal and Kaplan-Meier

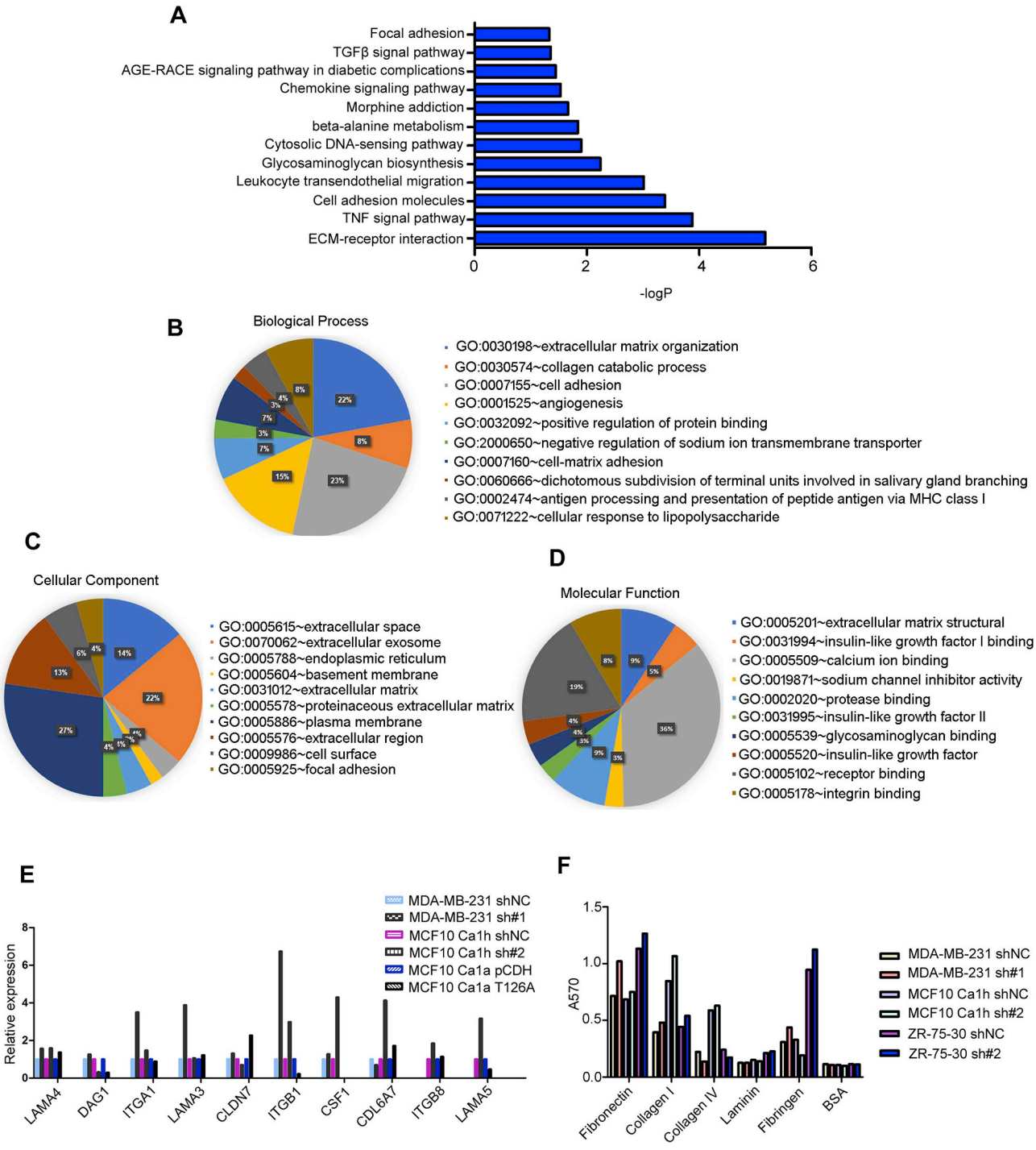

Fig. 4. Loss of TMEM126A increases the expression of extracellular matrix (ECM) molecules and enhances cell adhesion to the ECM.
A, The top 12 signaling pathways enriched based on the KEGG pathway analysis with the RNA sequence data from TMEM126A-knockdown MDA-MB-231 and TMEM126A-upregulated MCF10-Ca1a. B-D, The top 30 enriched Biological Processes, Molecular Functions, and Cellular Components based on the gene ontology analysis with the RNA sequence data from TMEM126A-knockdown MDA-MB-231 and TMEM126A-upregulated MCF10-Ca1a. E, mRNA expression of ECM molecules as assessed by real-time PCR. F, ECM adhesion assay in TMEM126A-depleted MDA-MB-231, MCF10-Ca1h, and ZR-75-30 cell lines.

plotter databases also indicated that TMEM126A expression is related to breast cancer prognosis (Fig. 1H and I). We also confirmed that the downregulation of TMEM126A in breast cancer cell lines is associated with significantly enhanced metastasis and that overexpression decreased the metastatic potential of cell lines (Fig. 3). Our results indicated that a better understanding of how TMEM126A regulates tumor invasion is essential to prevent their spread.

In mouse myeloid cells, TMEM126A has been reported to interact with CD137L and to be involved in CD137L reverse signal-mediated cellular responses [15,16]. CD137L, the ligand of CD137, is usually expressed on antigen presenting cells and a variety of solid tumor tissues and cell lines, including breast, colorectal, and lung cancers [20–22]. Due to bidirectional signaling of the CD137 receptor/ligand system [23], the activation of CD137 might not only elevate T and NK cell activities, but also affect the biological function of CD137L-expressing cells via reverse signaling [24,25]. In the present study, we

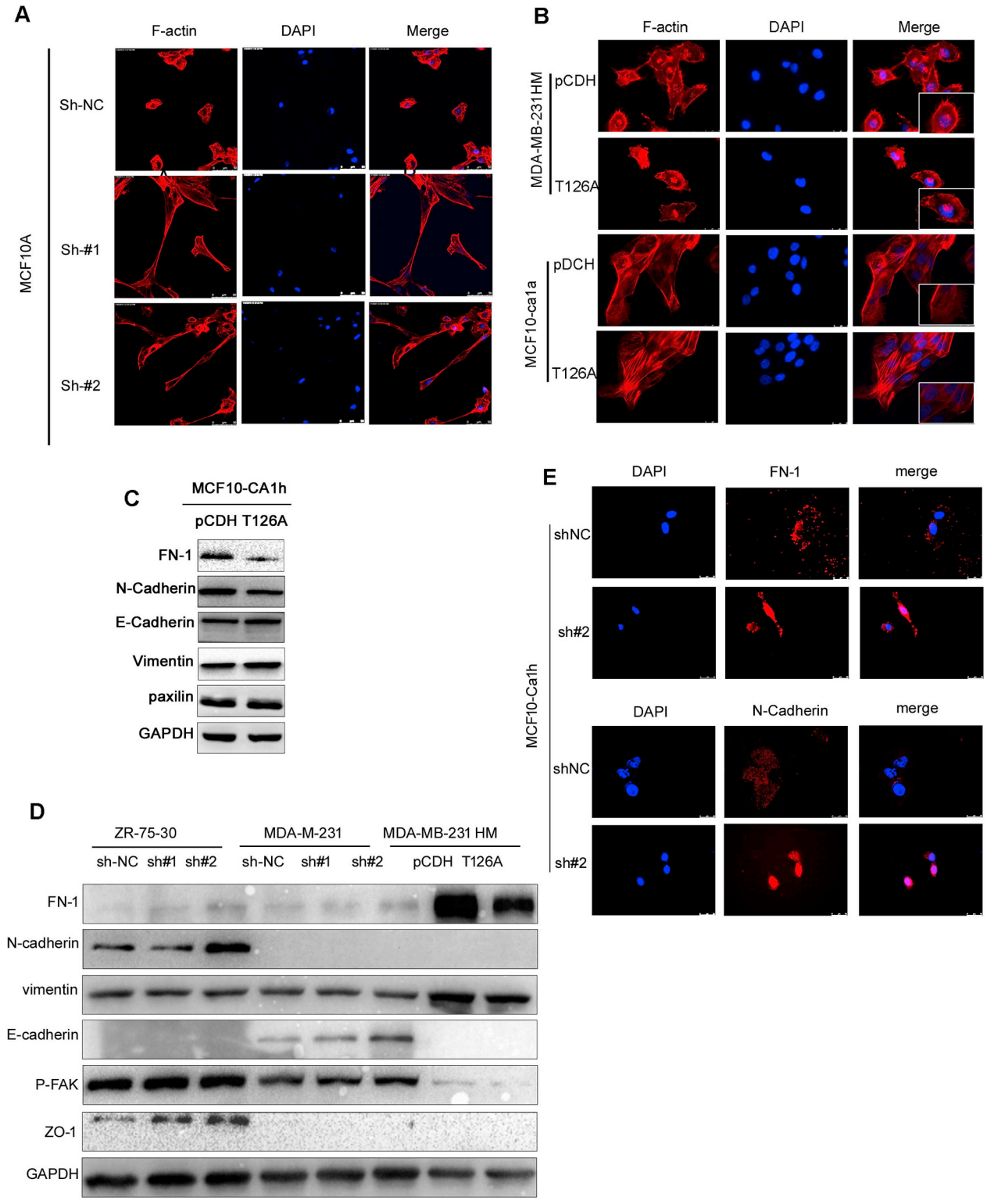

Fig. 5. Effect of TMEM126A downregulation on epithelial-to-mesenchymal transition.
A and B, F-actin staining of MCF10A (shNC vs. sh#1, sh#2), MDA-MB-231HM (pCDH vs. T126A), and MCF10-Ca1a (pCDH vs. T126A) cells based on immunofluorescence (IF). C and D, Expression of the EMT markers FN-1, N-cadherin, and vimentin in cell lines (MCF10-Ca1h, ZR-75-30, MDA-MB-231, and MDA-MB-231HM) after TMEM126A overexpression or downregulation based on western blotting. E: Expression of FN-1 and N-cadherin in MCF10-Ca1h TMEM126A-knockdown cells based on IF.

found that TMEM126A associates with CD137L in breast cancer. However, the activation of CD137L reverse signaling via CD137-Fc did not alter the expression of *p*-ERK and *p*-AKT when compared with that in IgG1-treated control cells. In addition, the isolation of membrane and cytoplasmic components suggested that TMEM126A knockdown did not change the location of CD137L (Supplementary Figs. S3A–E). These results indicate that the binding of TMEM126A to CD137L, as in immune cells, might have only a negligible effect on CD137L reverse

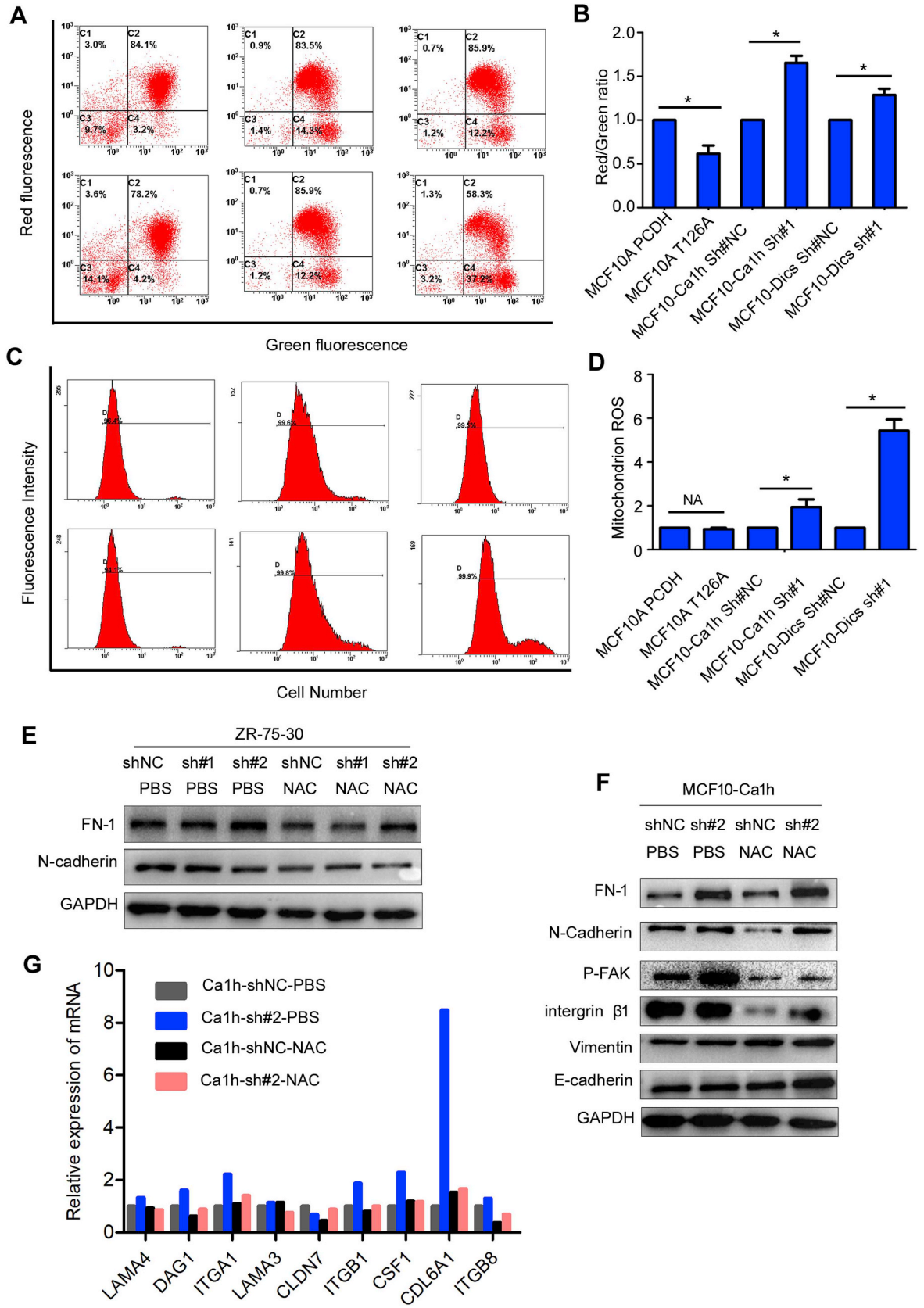

Fig. 6. ROS scavenger reverses TMEM126A-mediated epithelial-to-mesenchymal transition (EMT) and extracellular matrix (ECM) reprogramming.
A and B, Mitochondrial membrane potential (MMP) analysis in MCF10-Ca1h and MCF10-Dics cells after TMEM126A knockdown and in TMEM126A-overexpressing MCF10A cells. C and D, Mitochondrial reactive oxygen species (MtROS) analysis in MCF10-Ca1h and MCF10-Dics cells after TMEM126A knockdown and in TMEM126A-overexpressing MCF10A cells. E and F, Analysis of the expression of EMT markers after treatment with a ROS scavenger (10 mM NAC) for 24 h. G, Analysis of expression of ECM molecules after treatment with a ROS scavenger (10 mM NAC) for 24 h.

signaling.

Cancer cell invasion is the crucial primary step for metastasis. In this process, cells alter their cell-cell adhesion and attach to the ECM, which is mainly mediated by integrins [26]. The major constituents of the ECM are fibrous proteins, such as collagens, fibronectins, laminins, fibrinogen, and elastins, among others [27]. Excessive ECM deposition is associated with invasive carcinoma [28]. In the present study, we found that the downregulation of TMEM126A promotes the expression of LAMA4, DAG1, ITGA1, LAMA3, ITGB1, CSF1, and CDL6A7, thus promoting the adhesion of cells to ECM components, such as fibronectin, collagen I, collagen IV, and fibrinogen (Fig. 4F).

The initial process of cell invasion requires cells to escape from the primary tumor site, which depends on cell motility and migration. EMT might be the mechanism through which single tumor cells escape the epithelial tumor [29–31]. During EMT, tumor cells suppress the expression of epithelial-related genes such as E-cadherin and elevate mesenchymal-associated genes such as FN-1, N-cadherin, and vimentin, among others [32–34]. In the present study, the loss of TMEM126A expression significantly elevated the levels of FN-1 and N-cadherin, but only marginally altered the expression of E-cadherin (Fig. 5C and D). In addition, TMEM126A knockdown also induced actin cytoskeletal rearrangements (Fig. 5A and B).

*TMEM1*26A is a mitochondrial located mRNA (MLR) and the protein is anchored to the inner membrane, close to the cristae [12]. It has been reported that MLRs encoded by nuclear genes are localized and translated to the vicinity of the mitochondrial outer membrane and that the encoded proteins play vital roles during the early stages of mitochondrial complex biogenesis or constitute the core of mitochondrial respiratory complexes [35–37]. Therefore, we tried to understand whether TMEM126A affects mitochondrial biogenesis or mitochondrial respiration. We detected ATP production and ROS production after TMEM126A knockdown, and the results showed that TMEM126A marginally reduced the production of ATP (data not shown), and significantly caused the loss of MMP and increases ROS production in TMEM126A-downregulated cells. TMEM126A might participate in the regulation of mitochondrial respiratory complex assembly or the electron transport chain (ETC), thus suppressing the expression of TMEM126A resulting in partial ETC inhibition, subsequently leading to ROS overproduction. Some sporadic results have indicated that ROS decreases MMP by acting on thiols in the permeability transition pore complex to facilitate the opening of the complex and shifting the MMP [38–40].

Recent studies have indicated that mitochondria play a critical role in tumor metastasis via generation of ROS, decreases in MMP, metabolism disorder in mitochondria, and imbalances in mitochondrial fission and fusion [41–43]. The effect of ROS on tumor is dose-dependent; high concentrations induce apoptosis, whereas low concentrations promote cell proliferation and metastasis [44]. For example, some chemotherapeutic drugs induce cell death via ROS overproduction, whereas relatively low doses of ROS lead to mitochondrial dysfunction, promoting tumor metastasis; therefore, the use of an ROS scavenger can effectively inhibit metastasis [45]. In addition, ROS, as a secondary messenger, promote mitochondrial retrograde signaling to the nucleus by activating downstream effectors [46]. For example, mtROS can activate Src and Pyk2 to promote metastasis [45,47]. Rac1b-mediated increase in ROS stimulates the expression of Snail and EMT [48]. ROS also activate the NF-κB and AKT signaling pathways to promote tumor progression [49,50]. In the present study, an ROS scavenger significantly reduced the level of FN-1 and N-cadherin and suppressed the expression of ECM molecules, such as LAMA4, DAG1, ITGA1, LAMA3, ITGB1, CSF1, and CDL6A7 (Fig. 6E–G). These results suggest that ROS scavenging can significantly restore EMT and ECM remodeling. The results also indicate that the loss of TMEM126A might promote cell adhesion and metastasis by activating mitochondrial retrograde signaling. However, transcription factors activated by mtROS and the downstream processes initiated remain unknown.

In the present study, we observed that TMEM126A was downregulated in metastatic breast cancer and elucidated some of the downstream signal pathways. However, the upstream regulation mechanism of TMEM126A could not be elucidated. After predicting transcription factors that might bind to TMEM126A promoter, we found that some metastatic suppressors such as p53 [51] and FOXP3 [52,53] might regulate the transcription of TMEM126A. Further studies to explore the upstream regulation of TMEM126A, such as p53 and FOXP3, might help understand the reason why TMEM126A is downregulated in metastatic breast cancer.

In summary, to the best of our knowledge, the present study is the first to demonstrate that the mitochondrial inner membrane protein TMEM126A is a suppressor of breast cancer metastasis. TMEM126A depletion induces mtROS overproduction, leading to EMT by activating ECM remodeling. These findings might provide novel insights to identify prognostic indicators for patients with breast cancer.

Conflicts of interest

The authors declare no conflicts of interest.

Acknowledgements

This work was supported by grants from National Natural Science Foundation of China (81302299) and Shanghai Natural Science Foundation (17ZR1405800).

Appendix A. Supplementary data

Supplementary data to this article can be found online at https://doi.org/10.1016/j.canlet.2018.10.018.

References

[1] C.M. Perou, T. Sorlie, M.B. Eisen, M. van de Rijn, S.S. Jeffrey, C.A. Rees, J.R. Pollack, D.T. Ross, H. Johnsen, L.A. Akslen, O. Fluge, A. Pergamenschikov, C. Williams, S.X. Zhu, P.E. Lonning, A.L. Borresen-Dale, P.O. Brown, D. Botstein, Molecular portraits of human breast tumours, Nature 406 (2000) 747–752.
[2] B. Weigelt, J.L. Peterse, L.J. van 't Veer, Breast cancer metastasis: markers and models, Nat. Rev. Canc. 5 (2005) 591–602.
[3] D. Tang, M.T. Lotze, R. Kang, H.J. Zeh, Apoptosis promotes early tumorigenesis, Oncogene 30 (2010) 1851–1854.
[4] H.S. Kim, K. Patel, K. Muldoon-Jacobs, K.S. Bisht, N. Aykin-Burns, J.D. Pennington, R. van der Meer, P. Nguyen, J. Savage, K.M. Owens, A. Vassilopoulos, O. Ozden, S.H. Park, K.K. Singh, S.A. Abdulkadir, D.R. Spitz, C.X. Deng, D. Gius, SIRT3 is a mitochondria-localized tumor suppressor required for maintenance of mitochondrial integrity and metabolism during stress, Cancer Cell 17 (2010) 41–52.
[5] K. Ishikawa, K. Takenaga, M. Akimoto, N. Koshikawa, A. Yamaguchi, H. Imanishi, K. Nakada, Y. Honma, J. Hayashi, ROS-generating mitochondrial DNA mutations can regulate tumor cell metastasis, Science 320 (2008) 661–664.
[6] S. Vyas, E. Zaganjor, M.C. Haigis, Mitochondria and cancer, Cell 166 (2016) 555–566.
[7] H.L. Jiang, H.F. Sun, S.P. Gao, L.D. Li, X. Hu, J. Wu, W. Jin, Loss of RAB1B promotes triple-negative breast cancer metastasis by activating TGF-beta/SMAD signaling, Oncotarget 6 (2015) 16352–16365.
[8] H.L. Jiang, H.F. Sun, S.P. Gao, L.D. Li, S. Huang, X. Hu, S. Liu, J. Wu, Z.M. Shao, W. Jin, SSBP1 suppresses TGFbeta-driven epithelial-to-mesenchymal transition and metastasis in triple-negative breast cancer by regulating mitochondrial retrograde signaling, Can. Res. 76 (2016) 952–964.
[9] L.D. Li, H.F. Sun, X.X. Liu, S.P. Gao, H.L. Jiang, X. Hu, W. Jin, Down-regulation of NDUFB9 promotes breast cancer cell proliferation, metastasis by mediating mitochondrial metabolism, PLoS One 10 (2015) e0144441.
[10] S.P. Gao, H.F. Sun, H.L. Jiang, L.D. Li, X. Hu, X.E. Xu, W. Jin, Loss of COX5B inhibits proliferation and promotes senescence via mitochondrial dysfunction in breast cancer, Oncotarget 6 (2015) 43363–43374.
[11] S. Hanein, I. Perrault, O. Roche, S. Gerber, N. Khadom, M. Rio, N. Boddaert, M. Jean-Pierre, N. Brahimi, V. Serre, D. Chretien, N. Delphin, L. Fares-Taie, S. Lachheb, A. Rotig, F. Meire, A. Munnich, J.L. Dufier, J. Kaplan, J.M. Rozet, TMEM126A, encoding a mitochondrial protein, is mutated in autosomal-recessive nonsyndromic optic atrophy, Am. J. Hum. Genet. 84 (2009) 493–498.
[12] S. Hanein, M. Garcia, L. Fares-Taie, V. Serre, Y. De Keyzer, T. Delaveau, I. Perrault, N. Delphin, S. Gerber, A. Schmitt, J.M. Masse, A. Munnich, J. Kaplan, F. Devaux, J.M. Rozet, TMEM126A is a mitochondrial located mRNA (MLR) protein of the mitochondrial inner membrane, Biochim. Biophys. Acta 1830 (2013) 3719–3733.
[13] J. Desir, F. Coppieters, N. Van Regemorter, E. De Baere, M. Abramowicz,

M. Cordonnier, TMEM126A mutation in a Moroccan family with autosomal recessive optic atrophy, Mol. Vis. 18 (2012) 1849–1857.
[14] E. Meyer, M. Michaelides, L.J. Tee, A.G. Robson, F. Rahman, S. Pasha, L.M. Luxon, A.T. Moore, E.R. Maher, Nonsense mutation in TMEM126A causing autosomal recessive optic atrophy and auditory neuropathy, Mol. Vis. 16 (2010) 650–664.
[15] E.C. Kim, J.H. Moon, S.W. Kang, B. Kwon, H.W. Lee, TMEM126A, a CD137 ligand binding protein, couples with the TLR4 signal transduction pathway in macrophages, Mol. Immunol. 64 (2015) 244–251.
[16] J.S. Bae, J.K. Choi, J.H. Moon, E.C. Kim, M. Croft, H.W. Lee, Novel transmembrane protein 126A (TMEM126A) couples with CD137L reverse signals in myeloid cells, Cell. Signal. 24 (2012) 2227–2236.
[17] X. Xiao, L. Wang, P. Wei, Y. Chi, D. Li, Q. Wang, S. Ni, C. Tan, W. Sheng, M. Sun, X. Zhou, X. Du, Role of MUC20 overexpression as a predictor of recurrence and poor outcome in colorectal cancer, J. Transl. Med. 11 (2013) 151.
[18] Y.Z. Zheng, Z.G. Cao, X. Hu, Z.M. Shao, The endoplasmic reticulum stress markers GRP78 and CHOP predict disease-free survival and responsiveness to chemotherapy in breast cancer, Breast Canc. Res. Treat. 145 (2014) 349–358.
[19] A.J. Minn, G.P. Gupta, P.M. Siegel, P.D. Bos, W. Shu, D.D. Giri, A. Viale, A.B. Olshen, W.L. Gerald, J. Massague, Genes that mediate breast cancer metastasis to lung, Nature 436 (2005) 518–524.
[20] J. Dimberg, A. Hugander, D. Wagsater, Expression of CD137 and CD137 ligand in colorectal cancer patients, Oncol. Rep. 15 (2006) 1197–1200.
[21] H.R. Salih, S.G. Kosowski, V.F. Haluska, G.C. Starling, D.T. Loo, F. Lee, A.A. Aruffo, P.A. Trail, P.A. Kiener, Constitutive expression of functional 4-1BB (CD137) ligand on carcinoma cells, J. Immunol. 165 (2000) 2903–2910.
[22] Q. Wang, P. Zhang, Q. Zhang, X. Wang, J. Li, C. Ma, W. Sun, L. Zhang, Analysis of CD137 and CD137L expression in human primary tumor tissues, Croat. Med. J. 49 (2008) 192–200.
[23] H. Schwarz, Biological activities of reverse signal transduction through CD137 ligand, J. Leukoc. Biol. 77 (2005) 281–286.
[24] B. Dharmadhikari, M. Wu, N.S. Abdullah, S. Rajendran, N.D. Ishak, E. Nickles, Z. Harfuddin, H. Schwarz, CD137 and CD137L signals are main drivers of type 1, cell-mediated immune responses, OncoImmunology 5 (2016) e1113367.
[25] Y. Qian, D. Pei, T. Cheng, C. Wu, X. Pu, X. Chen, Y. Liu, H. Shen, W. Zhang, Y. Shu, CD137 ligand-mediated reverse signaling inhibits proliferation and induces apoptosis in non-small cell lung cancer, Med. Oncol. 32 (2015) 44.
[26] D.S. Harburger, D.A. Calderwood, Integrin signalling at a glance, J. Cell Sci. 122 (2009) 159–163.
[27] C. Frantz, K.M. Stewart, V.M. Weaver, The extracellular matrix at a glance, J. Cell Sci. 123 (2010) 4195–4200.
[28] M.P. Shekhar, R. Pauley, G. Heppner, Host microenvironment in breast cancer development: extracellular matrix-stromal cell contribution to neoplastic phenotype of epithelial cells in the breast, Breast Canc. Res. 5 (2003) 130–135.
[29] R. Kalluri, R.A. Weinberg, The basics of epithelial-mesenchymal transition, J. Clin. Invest. 119 (2009) 1420–1428.
[30] J. Yang, R.A. Weinberg, Epithelial-mesenchymal transition: at the crossroads of development and tumor metastasis, Dev. Cell 14 (2008) 818–829.
[31] J.P. Thiery, H. Acloque, R.Y. Huang, M.A. Nieto, Epithelial-mesenchymal transitions in development and disease, Cell 139 (2009) 871–890.
[32] M.K. Wendt, M.A. Taylor, B.J. Schiemann, W.P. Schiemann, Down-regulation of epithelial cadherin is required to initiate metastatic outgrowth of breast cancer, Mol. Biol. Cell 22 (2011) 2423–2435.
[33] B.E. Gould Rothberg, M.B. Bracken, E-cadherin immunohistochemical expression as a prognostic factor in infiltrating ductal carcinoma of the breast: a systematic review and meta-analysis, Breast Canc. Res. Treat. 100 (2006) 139–148.
[34] M. Yilmaz, G. Christofori, Mechanisms of motility in metastasizing cells, Mol. Canc. Res. 8 (2010) 629–642.
[35] M. Garcia, X. Darzacq, T. Delaveau, L. Jourdren, R.H. Singer, C. Jacq, Mitochondria-associated yeast mRNAs and the biogenesis of molecular complexes, Mol. Biol. Cell 18 (2007) 362–368.
[36] G. Lelandais, Y. Saint-Georges, C. Geneix, L. Al-Shikhley, G. Dujardin, C. Jacq, Spatio-temporal dynamics of yeast mitochondrial biogenesis: transcriptional and post-transcriptional mRNA oscillatory modules, PLoS Comput. Biol. 5 (2009) e1000409.
[37] S. Matsumoto, T. Uchiumi, T. Saito, M. Yagi, S. Takazaki, T. Kanki, D. Kang, Localization of mRNAs encoding human mitochondrial oxidative phosphorylation proteins, Mitochondrion 12 (2012) 391–398.
[38] B.B. Zhang, D.G. Wang, F.F. Guo, C. Xuan, Mitochondrial membrane potential and reactive oxygen species in cancer stem cells, Fam. Cancer 14 (2015) 19–23.
[39] J.J. Duivenvoorden, L.N. Bouman, F.F. Bukauskas, T. Opthof, H.J. Jongsma, Phase dependency of electrotonic spread of hyperpolarizing current pulses in the rabbit sinoatrial node, J. Mol. Cell. Cardiol. 22 (1990) 415–427.
[40] B.Y. Klein, I. Gal, M. Libergal, H. Ben-Bassat, Opposing effects on mitochondrial membrane potential by malonate and levamisole, whose effect on cell-mediated mineralization is antagonistic, J. Cell. Biochem. 60 (1996) 139–147.
[41] J. Zhao, J. Zhang, M. Yu, Y. Xie, Y. Huang, D.W. Wolff, P.W. Abel, Y. Tu, Mitochondrial dynamics regulates migration and invasion of breast cancer cells, Oncogene 32 (2013) 4814–4824.
[42] S.S. Sabharwal, P.T. Schumacker, Mitochondrial ROS in cancer: initiators, amplifiers or an Achilles' heel? Nat. Rev. Canc. 14 (2014) 709–721.
[43] M.V. Berridge, L. Dong, J. Neuzil, Mitochondrial DNA in tumor initiation, progression, and metastasis: role of horizontal mtDNA transfer, Can. Res. 75 (2015) 3203–3208.
[44] M.L. Verschoor, R. Ungard, A. Harbottle, J.P. Jakupciak, R.L. Parr, G. Singh, Mitochondria and cancer: past, present, and future, BioMed Res. Int. 2013 (2013) 612369.
[45] P.E. Porporato, V.L. Payen, J. Perez-Escuredo, C.J. De Saedeleer, P. Danhier, T. Copetti, S. Dhup, M. Tardy, T. Vazeille, C. Bouzin, O. Feron, C. Michiels, B. Gallez, P. Sonveaux, A mitochondrial switch promotes tumor metastasis, Cell Rep. 8 (2014) 754–766.
[46] R.K. Singh, A. Srivastava, P. Kalaiarasan, S. Manvati, R. Chopra, R.N. Bamezai, mtDNA germ line variation mediated ROS generates retrograde signaling and induces pro-cancerous metabolic features, Sci. Rep. 4 (2014) 6571.
[47] P.E. Porporato, P. Sonveaux, Paving the way for therapeutic prevention of tumor metastasis with agents targeting mitochondrial superoxide, Mol. Cell. Oncol. 2 (2015) e968043.
[48] D.C. Radisky, D.D. Levy, L.E. Littlepage, H. Liu, C.M. Nelson, J.E. Fata, D. Leake, E.L. Godden, D.G. Albertson, M.A. Nieto, Z. Werb, M.J. Bissell, Rac1b and reactive oxygen species mediate MMP-3-induced EMT and genomic instability, Nature 436 (2005) 123–127.
[49] J. Kwon, S.R. Lee, K.S. Yang, Y. Ahn, Y.J. Kim, E.R. Stadtman, S.G. Rhee, Reversible oxidation and inactivation of the tumor suppressor PTEN in cells stimulated with peptide growth factors, Proc. Natl. Acad. Sci. U. S. A 101 (2004) 16419–16424.
[50] N.S. Chandel, W.C. Trzyna, D.S. McClintock, P.T. Schumacker, Role of oxidants in NF-kappa B activation and TNF-alpha gene transcription induced by hypoxia and endotoxin, J. Immunol. 165 (2000) 1013–1021.
[51] E. Powell, D. Piwnica-Worms, H. Piwnica-Worms, Contribution of p53 to metastasis, Cancer Discov. 4 (2014) 405–414.
[52] A. Merlo, P. Casalini, M.L. Carcangiu, C. Malventano, T. Triulzi, S. Menard, E. Tagliabue, A. Balsari, FOXP3 expression and overall survival in breast cancer, J. Clin. Oncol. 27 (2009) 1746–1752.
[53] S. Douglass, S. Ali, A.P. Meeson, D. Browell, J.A. Kirby, The role of FOXP3 in the development and metastatic spread of breast cancer, Canc. Metastasis Rev 31 (2012) 843–854.